Adaptive evolution of nontransitive fitness in yeast

Sean W. Buskirk[1,2], Alecia B. Rokes[1], Gregory I. Lang[1]*

[1] Department of Biological Sciences, Lehigh University, Bethlehem PA 18015.

[2] Present Address: Department of Biology, West Chester University, West Chester PA 19383.

*Correspondence: glang@lehigh.edu

Abstract

Nontransitivity – commonly illustrated by the rock-paper-scissors game – is well documented among extant species as a contributor to biodiversity. However, it is unclear if nontransitive interactions also arise by way of genealogical succession, and if so, through what mechanisms. Here we identify a nontransitive evolutionary sequence in the context of yeast experimental evolution in which a 1,000-generation evolved clone outcompetes a recent ancestor but loses in direct competition with a distant ancestor. We show that nontransitivity arises due to the combined forces of adaptation in the yeast nuclear genome and the stepwise deterioration of an intracellular virus. We show that, given the initial conditions of the experiment, this outcome likely to arise: nearly half of all populations experience multilevel selection, fixing adaptive mutations in both the nuclear and viral genomes. In contrast to conventional views of virus-host coevolution, we find no evidence that viral mutations (including loss of the virus) increase the fitness of the host. Instead, the evolutionary success of evolved viral variants results from their selective advantage over viral competitors within the context of individual cells. Our results provide the first mechanistic case-study of the adaptive evolution of nontransitivity, in which a series of adaptive replacements produce organisms that are less fit when compared to a distant genealogical ancestor.

Introduction

Adaptive evolution is a process in which selective events result in the replacement of less-fit genotypes with a more fit ones. Intuitively, a series of selective events, each improving fitness relative to the immediate predecessor, should translate into a cumulative increase in fitness relative to the ancestral state. However, whether or not this is borne out over long evolutionary time scales has long been the subject of debate (Ruse 1993, Dawkins 1997, Gould 1997, Shanahan 2000). The failure to identify broad patterns of progress over evolutionary time scales—despite clear evidence of selection acting over successive short time intervals—is what Gould referred to as "the paradox of the first tier (Gould 1985)." This paradox implies that evolution exhibits nontransitivity, a property that is best illustrated by the Penrose staircase and the Rock-Paper-Scissors game. The Penrose staircase is a visual illusion of ascending sets of stairs that form a continuous loop such that—although each step appears higher than the last—no upward movement is realized. In the Rock-Paper-Scissors game each two-way interaction has a clear winner (paper beats rock, scissors beats paper, and rock beats scissors), yet due to the nontransitivity of these two-way interactions, no clear hierarchy exists among the three.

In ecology, nontransitive interactions among extant species are well-documented as contributors to biological diversity and community structure (Kerr et al. 2002, Károlyi et al. 2005, Laird and Schamp 2006, Reichenbach et al. 2007, Menezes et al. 2019) and arise by way of resource (Sinervo and Lively 1996, Precoda et al. 2017) or interference competition (Kirkup and Riley 2004). First put forward in the 1970s (Gilpin 1975, Jackson and Buss 1975, May and Leonard 1975, Petraitis 1979), the importance of nontransitivity in ecology has garnered extensive theoretical and experimental consideration over the last half century (e.g. Sinervo and Lively 1996, Kerr et al. 2002, Allesina and Levine 2011, Rojas-Echenique and Allesina 2011, Soliveres et al. 2015, Liao et al. 2019).

What is unknown is whether nontransitive interactions arise for direct descendants along a line of genealogical succession. This is the crux of Gould's paradox and has broad implications for our understanding of evolutionary processes. For instance, if an evolved genotype is found to be less fit in

51 comparison to a distant ancestor, the adaptive landscape upon which the population is evolving may not
52 contain true fitness maxima (Barrick and Lenski 2013, Van den Bergh et al. 2018) and, more broadly,
53 directionality and progress may be illusory (Gould 1996). Testing the hypothesis that nontransitive
54 interactions arise along lines of genealogical descent, however, is not possible in natural populations
55 because it requires our ability to directly compete an organism against its immediate predecessor as well
56 as against its extinct genealogical ancestors. Fortunately, laboratory experimental evolution, in which
57 populations are preserved as a "frozen fossil record," affords us with the unique opportunity to test for
58 nontransitivity along a genealogical lineage by directly competing a given genotype against the extant as
59 well as the extinct.

60 An early study of laboratory evolution of yeast in glucose-limited chemostats appeared to
61 demonstrate that nontransitive interactions arise along a line of genealogical descent (Paquin and Adams
62 1983). However, the specific events that led to nontransitivity in this case are unknown, and it is likely the
63 case that the authors were measuring interactions between contemporaneous lineages in a population,
64 rather than individuals along a direct line of genealogical descent, as they report (see Discussion). Indeed,
65 adaptive diversification is common in experimental evolution due to spatial structuring (Rainey and
66 Travisano 1998, Frenkel et al. 2015) and metabolic diversification (Helling et al. 1987, Turner et al. 1996,
67 Spencer et al. 2008, Plucain et al. 2014), and is typically maintained by negative frequency-dependent
68 selection, in which rare genotypes are favored. Collectively this work reinforces theory and observational
69 evidence on the power of ecological nontransitivity as a driver and maintainer of diversity but is silent as
70 to whether genealogical succession can also be nontransitive.

71 Here we determine the sequence of events leading to the evolution of nontransitivity in a single
72 yeast population during a 1,000-generation evolution experiment. We show that nontransitivity arises
73 through multilevel selection involving both the yeast nuclear genome and the population of a vertically-
74 transmitted virus. Many fungi, including the yeast *Saccharomyces cerevisiae* are host to non-infectious,
75 double-stranded RNA "killer" viruses (Wickner 1976, Schmitt and Breinig 2002, Schmitt and Breinig
76 2006, Rowley 2017). Killer viruses produce a toxin that kills non-killer containing yeasts. The K1 toxin

77 gene contains four subunits (δ, α, γ, β), which are post-translationally processed and glycosylated to
78 produce an active two-subunit (α, β) secreted toxin (Bostian et al. 1983). Immunity to the toxin is
79 conferred by the pre-processed version of the toxin, thus requiring cells to maintain the virus for
80 protection. We show that nontransitivity arises due to multilevel selection: adaptation in the yeast nuclear
81 genome and the simultaneous stepwise deterioration of the killer virus. By expanding our study of host-
82 virus genome evolution to over 100 additional yeast populations, we find that multilevel selection, and
83 thus the potential for the evolution of nontransitive interactions, is a common occurrence given the
84 conditions of our evolution experiment.
85

86 ## Results

87 **Evolution of nontransivity along a line of genealogical descent**

88 Previously we evolved ~600 haploid populations of yeast asexually for 1,000 generations in rich
89 glucose medium (Lang et al. 2011). We characterized extensively the nuclear basis of adaptation for a
90 subset of these populations through whole-genome whole-population time-course sequencing (Lang et al.
91 2013) and/or fitness quantification of individual mutations (Buskirk et al. 2017).

92 For one population (BYS1-D08) we were surprised to observe that a 1,000-generation clone lost
93 in direct competition with a fluorescently-labeled version of the ancestor. To test the hypothesis that a
94 nontransitive interaction arose during the adaptive evolution of this population, we isolated individual
95 clones from three timepoints (Fig. 1A). We define these as Early (Generation 0), Intermediate
96 (Generation 335, chosen to coincide with the first clonal replacement, which fixes first three nuclear
97 mutations), and Late (Generation 1,000, following three additional clonal replacements, which fix ten
98 nuclear mutations). We performed pairwise competition experiments between the Early, Intermediate, and
99 Late clones at multiple starting frequencies. We find that the Intermediate clone is 3.8% more fit relative
100 to the Early clone and that the Late clone is 1.2% more fit relative to the Intermediate clone (Fig. 1B, left
101 panel). The expectation, assuming additivity, is that the Late clone will be more fit than the Early clone,

102 by roughly 5.0%. Surprisingly, we find that the Late clone is less fit than expected, to the extent that it
103 often loses in pairwise competition with the Early clone (Fig. 1B, left panel). Furthermore, the interaction
104 between the Early and Late clones exhibits positive frequency-dependent selection, thus creating a bi-
105 stable system where the fitness disadvantage of the Late clone can be overcome if it starts above a certain
106 frequency relative to the Early clone (Fig. S1).
107
108 **Evolution of nontransitivity is associated with changes to the killer virus**
109 Positive frequency-dependent selection is rare in experimental evolution and can only arise
110 throught a few known mechanisms. It has been observed previously in yeast that harbor killer viruses
111 (Greig and Travisano 2008), which are dsRNA viruses that encode toxin/immunity systems. Using a well-
112 described halo assay (Woods and Bevan 1968), we find that the ancestral strain of our evolved
113 populations exhibits the phenotype expected of yeast that harbor the killer virus: it inhibits growth of a
114 nearby sensitive strain and resists killing by a known killer strain (Fig. S2). By RT-PCR and sequencing
115 we find that our ancestral strain, which was derived from the common lab strain W303-1a, contains the
116 M1-type killer virus (encoding the K1-type killer toxin) with only minor differences from previously
117 sequenced strains (Fig. S3). In the ancestor we also detect the L-A helper virus, which supplies the RNA-
118 dependent RNA polymerase and capsid protein necessary for the killer virus, a satellite virus, to complete
119 its life cycle (Ribas and Wickner 1992).
120 We asked if the observed nontransitivity in the BYS1-D08 lineage could be explained by
121 evolution of the killer phenotype. Phenotyping of the isolated clones revealed that the Intermediate clone
122 no longer exhibits killing ability (K^-I^+) and that the Late clone possesses neither killing ability nor
123 immunity (K^-I^-, Fig. 1A, Fig. S4). Killer toxin has been shown to impart frequency-dependent selection in
124 structured environments (Greig and Travisano 2008) and we hypothesized that a stepwise loss of the
125 killer phenotypes was responsible for the frequency-dependent and nontransitive interaction between
126 Early and Late clones. To determine if the presence of the killer virus in the early clone is necessary for
127 the evolution of nontransitivity, we cured the Early clone and found that the Late clone was 4.3% more fit

128 than the killer-cured Early clone, with no correlation between fitness and frequency (Fig. 1B, right panel)
129 showing that the presence of killer virus in the Early clone is necessary for frequency-dependence and
130 nontransitivity. To determine if viral evolution alone is sufficient to account for the observed fitness gains
131 in nontransitive interactions, we transferred the killer virus from the Intermediate clone to the cured Early
132 clone and assayed fitness relative to the Early clone (Fig. 1B, right panel). We find that the evolved killer
133 virus confers no significant effect on host fitness. Therefore, changes to the killer virus alone are not
134 sufficient to account for the adaptive evolution of nontransitivity in this population, which must involve
135 changes to both the host and viral genomes.
136
137 **Changes to killer-associated phenotypes are common under our experimental conditions**
138 To determine the extent of killer phenotype evolution across all populations, we assayed the killer
139 phenotype of 142 populations that were founded by a single ancestor and propagated at the same
140 bottleneck size as BYS1-D08 (Lang et al. 2011). We find that approximately half of all populations
141 exhibit a loss or weakening of killing ability by Generation 1,000, with ~10% of populations exhibit
142 neither killing ability nor immunity (Fig. 2A, Fig. 2B). Of note, we did not observe loss of immunity
143 without loss of killing ability, an increase in killing ability or immunity, or reappearance of killing ability
144 or immunity once it was lost from a population (Fig. S5), apart from the noise associated with scoring of
145 population-level phenotypes. Several populations (i.e. BYS2-B09 and BYS2-B12) lost both killing ability
146 and immunity simultaneously, suggesting that a single event can cause the loss of both the killer
147 phenotypes.
148 Mutations in nuclear genes can affect killer-assiciated phenotypes. The primary receptors of the
149 K1 killer toxin are β-glucans in the yeast cell wall (Pieczynska et al. 2013). We observe a statistical
150 enrichment of mutations in genes involved in β-glucan biosynthesis (6-fold Gene Ontology (GO)
151 Biological Process enrichment, $P<0.0001$). Furthermore, of the 714 protein-coding mutations dispersed
152 across 548 genes, 40 occur within 11 of the 36 genes (identified by (Pagé et al. 2003)) that, when deleted,
153 confer a high level of resistance to the K1 toxin ($\chi^2=18.4$, $df=1$, $P=1.8\text{x}10^{-5}$). Nevertheless, the presence of

154 mutations in nuclear genes that have been associated with high levels of resistance is not sufficient to
155 account for the loss of killing ability (χ^2=1.037, *df*=1, *P*=0.309) or immunity (χ^2=0.103, *df*=1, *P*=0.748).
156
157 **Standing genetic variation and *de novo* mutations drive phenotypic change**
158 We sequenced viral genomes from a subset of yeast populations (n=67) at Generation 1,000, 57
159 of which change killer phenotype and 10 control populations that retained the ancestral killer phenotypes.
160 Viral genomes isolated from populations that lost killing ability possess 1-3 mutations in the M1 coding
161 sequence – most being missense variants (Fig. 3A). In contrast, only a single mutation, synonymous
162 nonetheless, was detected in M1 across the 10 control populations that retained the killer phenotype
163 (χ^2=59.3, *df*=1, *P*=1.4x10^{-13}). The correlation between the presence of mutations in the viral genome and
164 the loss of killing ability is strong evidence that viral mutations are responsible for the changes in killer
165 phenotypes. We estimate that by Generation 1,000 half of all populations have fixed viral variants that
166 alter killer phenotypes (for comparison, *IRA1*, the most common nuclear target, fixed in ~25% of
167 populations over the same time period).
168 Of the 57 populations that lost killing ability, 42 fixed one of three single nucleotide
169 polymorphisms, resulting in amino acid substitutions D106G, D253N, and I292M and observed 13, 14,
170 and 15 times, respectively (Table S1). Given their prevalence, these polymorphisms likely existed at low
171 frequency in the shared ancestral culture (indeed, we can detect one of the common polymorphisms,
172 D106G, in individual clones at the Early time point, indicating that this mutation was heteroplasmic in
173 cells of the founding population). Killer phenotypes are consistent across populations that fixed a
174 particular ancestral polymorphism (Table S1).
175 In addition to the three ancestral polymorphisms, we detect 34 putative *de novo* point mutations
176 that arose during the evolution of individual populations (Table S1). Mutations are localized to the K1
177 coding sequence, scattered across the four encoded subunits, and skewed towards missense mutations
178 relative to nonsense or frameshift (Fig. 3B). Fourteen of the seventy-eight identified mutations are
179 predicted to fall at or near sites of protease cleavage or post-translational modification necessary for toxin

180 maturation. Overall, however, the K1 coding sequence appears to be under balancing selection
181 (dN/dS=0.90), indicating that certain amino acid substitutions (e.g. those that eliminate immunity but
182 retain killing ability) are not tolerated. In addition, substitutions are extremely biased toward transitions
183 over transversions (Table S2, R=6.4, χ^2=44.2, df=1, P<0.0001), a bias that is also present in other
184 laboratory-derived M1 variants (R=4.1) (Suzuki et al. 2015) and natural variation of the helper L-A virus
185 (R=3.0) (Diamond et al. 1989, Icho and Wickner 1989). The transition:transversion bias appears specific
186 to viral genomes as the ratio is much lower within evolved nuclear genomes (R=0.8), especially in genes
187 inferred to be under selection (R=0.5), suggesting a mutational bias of the viral RNA-dependent RNA
188 polymerase (Lang et al. 2013, Fisher et al. 2018, Marad et al. 2018).
189 Though point mutations are the most common form of evolved variation, we also detected two
190 viral genomes in which large portions of the K1 ORF are deleted (Fig. 3B). Despite the loss of the
191 majority of the K1 coding sequence, the deletion mutants maintain cis signals for replication and
192 packaging (Ribas and Wickner 1992, Ribas et al. 1994). Notably, the two populations that possess these
193 deletion mutants also possess full-length viral variants. The deletion mutants we observe are similar to the
194 ScV-S defective interfering particles that have been shown to outcompete full-length virus presumably
195 due to their decreased replication time (Kane et al. 1979, Ridley and Wickner 1983, Esteban and Wickner
196 1988).
197
198 **Host/virus co-evolutionary dynamics are complex and operate over multiple scales**
199 To compare the dynamics of viral genome evolution, nuclear genome evolution, and phenotypic
200 evolution we performed time-course sequencing of viral genomes from three yeast populations that lost
201 killing ability and for which we have whole-population, whole-genome, time-course sequencing data for
202 the nuclear genome (Lang et al. 2013). As with the evolutionary dynamics of the host genome, the
203 dynamics of viral genome evolution feature clonal interference (competition between mutant genotypes),
204 genetic hitchhiking (an increase in frequency of an allele due to genetic linkage to a beneficial mutation),
205 and sequential sweeps (Fig. 4, Fig. S6). Interestingly, viral sweeps often coincide with nuclear sweeps.

206 Since the coinciding nuclear sweeps often contain known driver mutations, it is possible that the viral
207 variants themselves are not driving adaptation but instead hitchhiking on the back of beneficial nuclear
208 mutations. This is consistent with the observation that the introduction of the viral variant from the
209 Intermediate clone did not affect the fitness of the Early clone (Fig. 1B)

210 To determine if the loss of killer phenotype is caused solely by mutations in the killer virus, we
211 transferred the ancestral virus and five evolved viral variants to a virus-cured ancestor via cytoduction. Of
212 the five viral variants one exhibited weak killing ability and full immunity (D253N), three exhibited no
213 killing ability and full immunity (P47S, D106G, I292M), and one exhibited neither killing ability nor
214 immunity (-1 frameshift). For each viral variant, the killer phenotype of the cytoductant matched the killer
215 phenotype of the population of origin demonstrating that viral mutations are sufficient to explain changes
216 in killer phenotype (Fig. S7). To determine if any viral variants affect host fitness, we competed all five
217 cytoductants against the ancestor or a virus-cured ancestor in a pairwise manner. In competitions in which
218 both competitors shared either killing ability or immunity, no viral variants impacted host fitness;
219 therefore, production of active toxin or maintenance of the virus has no detectable fitness cost to the host
220 (Fig. 5A). In contrast, an incompatibility in the killer phenotype – produced by the simultaneous loss of
221 both killing ability and immunity – results in frequency dependent fitness interactions between competing
222 populations. Collectively, these pairwise competitions show that a stepwise degradation of the killer virus
223 is a neutral process and no evidence that host fitness is driving the loss of killer phenotype. These findings
224 support previous theoretical and empirical studies (Pieczynska et al. 2016, Pieczynska et al. 2017) that
225 claim that mycoviruses and their hosts have co-evolved to minimize cost.

226

227 **Success of evolved viral variants is due to an intracellular fitness advantage**

228 Based on the lack of a measurable effect of viral mutations on host fitness, we hypothesized that
229 the evolved viral variants may have a selective advantage within the viral population of individual yeast
230 cells. A within-cell advantage has been invoked to explain the invasion of internal deletion variants (e.g.
231 ScV-S (Kane et al. 1979)) but has not been extended to point mutations. To test evolved viral variants for

232 a within-cell fitness advantage, we generated a heteroplasmic diploid strain by mating the ancestor (with
233 wildtype virus) with a haploid cytoductant containing either the I292M (K^-I^+) or -1 frameshift (K^-I^-) viral
234 variant. The heteroplasmic diploids were propagated for seven single-cell bottlenecks every 48 hours to
235 minimize among-cell selection. At each bottleneck, we assayed the yeast cells for killer phenotypes and
236 we quantified the ratio of the intracellular viral variants by RT-PCR and sequencing. We find that killing
237 ability was lost from all lines, suggesting that the evolved viral variants outcompeted the ancestral variant
238 (Fig. 5B). Sequencing confirmed that the derived viral variant fixed in most lines (Fig. 5C). In some lines,
239 however, the derived viral variant increased initially before decreasing late. Further investigation into one
240 of these lines revealed that the decrease in frequency of the viral variant corresponded to the sweep of a
241 *de novo* G131D variant (Fig. 5C, inset). Viral variants therefore appear to constantly arise, and the
242 evolutionary success of the observed variants results from their selective advantage over viral competitors
243 within the context of an individual cell. We speculate that an intracellular competition between newly
244 arising viral variants also explains the loss of immunity from populations that previously lost killing
245 ability (Fig. S5), given the relaxed selection for the maintenance of functional immunity in those
246 populations.
247

248 ## Discussion

249 We examined phenotypic and sequence co-evolution of an intracellular double-stranded RNA
250 virus and the host nuclear genome over the course of 1,000 generations of experimental evolution. We
251 observe complex dynamics including genetic hitchhiking and clonal interference in the host populations
252 as well as the intracellular viral populations. Phenotypic and genotypic changes including the loss of
253 killing ability, mutations in the host-encoded cell-wall biosynthesis genes, and the virally encoded toxin
254 genes occur repeatedly across replicate populations. The loss of killer-associated phenotypes—killing
255 ability and immunity to the killer toxin—leads to three phenomena with implications for adaptive
256 evolution: positive frequency-dependent selection, multilevel selection, and nontransitivity.

257 Frequency-dependent selection can be either negative, where rare genotypes are favored, or
258 positive, where rare genotypes are disfavored. Of the two, negative frequency-dependent selection is more
259 commonly observed in experimental evolution, arising, for example, from cross-feeding between acetate
260 producers and consumers (Helling et al. 1987, Turner et al. 1996, Spencer et al. 2008, Plucain et al. 2014)
261 and spatial structuring in static environments (Rainey and Travisano 1998, Frenkel et al. 2015). Positive
262 frequency-dependent selection, in contrast, is not typically observed in experimental evolution. By
263 definition, a new positive frequency-dependent mutation must invade an established population at a time
264 when its fitness is at its minimum. Even in situations in which positive frequency-dependent selection is
265 likely to occur, such as the evolution of cooperative group behaviors and interference competition (Chao
266 and Levin 1981), a mutation may be unfavorable at the time it arises. A crowded, structured environment
267 provides an opportunity for allelopathies to offer a local advantage. Here we describe an alternative
268 mechanism for the success of positive frequency-dependent mutations through multilevel selection of the
269 host genome and a toxin-encoding intracellular virus. The likelihood of such a scenario occurring is aided
270 by the large population size of the extrachromosomal element: each of the ~10^5 cells that comprise each
271 yeast population contains ~10^2 viral particles (Bostian et al. 1983, Ridley and Wickner 1983).
272 Nontransitivity in our experimental system is due, in part, to interference competition: the
273 production of a killer toxin that kills non-killer-containing cells. Interference competition can drive
274 ecological nontransitivity (Kerr et al. 2002, Kirkup and Riley 2004), suggesting that similar mechanisms
275 may underlie both ecological and genealogical nontransitivity. The adaptive evolution of genealogical
276 nontransitivity in our system does not follow the canonical model of a co-evolutionary arms race where
277 the host evolves mechanisms to prevent the selfish replication of the virus and the virus evolves to
278 circumvent the host's defenses (Daugherty and Malik 2012, Rowley 2017). Rather, mutations that fix in
279 the viral and yeast populations do so because they provide a direct fitness advantage in their respective
280 populations. Nontransitivity arises through the combined effect of beneficial mutations in the host
281 genome (which improves the relative fitness within the yeast population, regardless of the presence or
282 absence of the killer virus) and the adaptive loss of killing ability and degeneration of the intracellular

283 virus (which provides an intracellular fitness advantage to the virus). The end result is a high-fitness yeast
284 genotype (relative to the ancestral yeast genotype) that contains degenerate viruses, rendering their hosts
285 susceptible to the virally-encoded toxin.

286 Though we did not find an impact of nuclear mutations on killer-associated phenotypes, we do
287 observe a statistical enrichment of mutations in genes involved in β-glucan biosynthesis and in genes that
288 when deleted confer a high level of resistance to the killer toxin. Nearly all mutations in these toxin-
289 resistance genes are nonsynonymous (18 nonsense/frameshift, 21 missense, 1 synonymous), indicating a
290 strong signature of positive selection. This suggests that the nuclear genome adapting in response to the
291 presence of the killer toxin, however, the effect of these mutations may be beyond the resolution of our
292 fitness assay.

293 Among the viral variants, we identified were two unique ~1 kb deletions; remnants of the killer
294 virus that retain little more than the *cis*-acting elements necessary for viral replication and packaging.
295 These defective interfering particles are thought to outcompete full-length virus due to their decreased
296 replication time (Kane et al. 1979, Ridley and Wickner 1983, Esteban and Wickner 1988). Defective
297 interfering particles are common to RNA viruses (Holland et al. 1982). Though there are several different
298 killer viruses in yeast (e.g. K1, K2, K28, Klus), each arose independently and has a distinct mechanism of
299 action (Rodríguez-Cousiño et al. 2017). Nontransitive interactions may therefore arise frequently through
300 cycles of gains and losses of toxin production and toxin immunity in lineages that contain RNA viruses.

301 Reports of nontransitivity arising along evolutionary lines of descent are rare (de Visser and
302 Lenski 2002, Beaumont et al. 2009). The first (and most widely cited) report of nontransitivity along a
303 direct line of descent occurred during yeast adaptation in glucose-limited chemostats (Paquin and Adams
304 1983). This experiment was correctly interpreted under the assumption—generally accepted at the time—
305 that large asexual populations evolved by clonal replacement. This strong selection/weak mutation model,
306 however, is now known to be an oversimplification for large asexual populations, where multiple
307 beneficial mutations arise and spread simultaneously through the population (Gerrish and Lenski 1998,
308 Kvitek and Sherlock 2013, Lang et al. 2013). In addition, the duration of the Paquin and Adams

experiment was too short for the number of reported selective sweeps to have occurred (four in 245 generations and six in 305 generations, for haploids and diploids, respectively). The strongest known beneficial mutations in glucose-limited chemostats, hexose transporter amplifications, provide a fitness advantage of ~30% (Gresham et al. 2008, Kvitek and Sherlock 2011) and would require a minimum of ~150 generations to fix in a population size of 4 x 10^9 (Otto and Whitlock 1997). We contend that Paquin and Adams observed nontransitive interactions among contemporaneous lineages—ecological nontransitivity—rather than nontransitivity among genealogical descendants. Apart from the present study, there are no other examples of nontransitivity arising along a line descent, but numerous examples of nontransitive interactions among contemporaneous lineages (Sinervo and Lively 1996, Kerr et al. 2002, Kirkup and Riley 2004, Károlyi et al. 2005, Laird and Schamp 2006, Reichenbach et al. 2007, Precoda et al. 2017, Menezes et al. 2019).

Here we present a mechanistic case study on the evolution of nontransitivity along a direct line of genealogical descent, and we determine the specific genetic events that lead to nontransitivity in one focal population. Our results show that the continuous action of selection can give rise to genotypes that are less fit compared to a distant ancestor. We show that nontransitive interactions can arise quickly due to multilevel selection in a host/virus system. In the context of this experiment multi-level selection is common—most yeast populations fix nuclear and viral variants by Generation 1,000. Overall, our results demonstrate that adaptive evolution is capable of giving rise to nontransitive fitness interactions along an evolutionary lineage, even under simple laboratory conditions.

Acknowledgments: We thank Reed Wickner, Amber Rice, and members of the Lang Lab for their comments on the manuscript. This work was supported by the NIH grant 1R01GM127420. Illumina data of viral competitions and evolved nuclear genomes are accessible under the BioProject ID PRJNA553562 and PRJNA205542, respectively. Conceptualization and writing were performed by S.W.B. and G.I.L. Investigation was performed by S.W.B. and A.B.R.

334 # Methods

335 Growth Conditions and Strain Construction

336 Unless specified otherwise, yeast strains were propagated at 30°C in YPD + A&T (yeast extract,
337 peptone, dextrose plus 100 μg/ml ampicillin and 25 μg/ml tetracycline to prevent bacterial
338 contamination).

339 The ancestor and evolved populations were described previously (Lang et al. 2011). Early,
340 Intermediate, and Late clones were isolated by resurrecting population BYS1-D08 at the Generation 0,
341 335, and 1,000, respectively. These specific timeponts were selected to coincide with the completion of a
342 selective sweep (Lang et al. 2013), when the population is expected to be near clonal. For each timepoint
343 we isolated multiple clones from a YPD plate and assayed each one to verify that the killer phenotype was
344 uniform.

345 The ancestral strain was cured of the M1 and LA viruses by streaking to single colonies on YPD
346 agar and confirmed by halo assay, PCR, and sequencing. We integrated a constitutively-expressed
347 fluorescent reporter (pACT1-ymCitrine) at the *CAN1* locus in the cured ancestral strain as well as the
348 Intermediate (Generation 335) and Late (Generation 1,000) clones.

349 Karyogamy mutants were constructed by introducing the *kar1Δ15* allele by two-step gene
350 replacement in the cured a *MAT*α version of the ancestor (Georgieva and Rothstein 2002). The *kar1Δ15*-
351 containing plasmid pMR1593 (Mark Rose, Georgetown University) was linearized with BglII prior to
352 transformation and selection on -Ura. Mitotic excision of the integrated plasmid was selected for plating
353 on 5-fluorotic acid (5-FOA). Then we perform replaced NatMX with KanMX to enable selection for
354 recipients during viral transfer.

355 Fitness Assays

356 Competitive fitness assays were performed as described previously (Lang et al. 2011, Lang et al.
357 2013). To investigate frequency dependence, competitors were mixed at various ratios at the initiation of
358 the experiment. Competitions were performed for 50 generations under conditions identical to the

359 evolution experiment (Lang et al. 2011). Every 10 generations, competitions were diluted 1:1,000 in fresh
360 media and an aliquot was sampled by BD FACS Canto II flow cytometer. Flow cytometry data was
361 analyzed using FlowJo 10.3. Relative fitness was calculated as the slope of the change in the natural log
362 ratio between the experimental and reference strain. To detect frequency-dependent selection, each 10-
363 generation interval was analyzed independently to calculate starting frequency and fitness.

364 Halo Assay

365 Killer phenotype was measured using a high-throughput version of the standard halo assay
366 (Crabtree et al. 2019) and a liquid handler (Biomek FX). Assays were performed using YPD agar that had
367 been buffered to pH 4.5 (citrate-phosphate buffer), dyed with methylene blue (0.003%), and poured into a
368 1-well rectangular cell culture plate.

369 Killing ability was assayed against a sensitive tester strain (yGIL1063) that was isolated from a
370 separate evolution experiment initiated from the same ancestor. The sensitive tester was grown to
371 saturation, diluted 1:10, and spread (150 µL) evenly on the buffered agar. Query strains were grown to
372 saturation, concentrated 5x, and spotted (2 µL) on top of the absorbed lawn (Fig. S2, left).

373 Immunity was assayed against the ancestral strain (yGIL432). Query strains were grown to
374 saturation, diluted 1:32, and spotted (10 µL) on the buffered agar. The killer tester was grown to
375 saturation, concentrated 5x, and spotted (2 µL) on top of the absorbed query strain (Fig. S2, right).
376 Plates were incubated at room temperature for 2-3 days before assessment. Killer phenotype was scored
377 according to the scale in shown in Fig. 2.

378 Viral RNA Isolation, cDNA Synthesis, PCR

379 Nucleic acids were isolated by phenol-chloroform extraction and precipitated in ethanol. Isolated
380 RNA was reverse-transcribed into cDNA using ProtoScript II First Strand cDNA Synthesis Kit (NEB)
381 with either the enclosed Random Primer Mix or the M1-specific oligo M1_R3 (Table S3).

382 Sanger Sequencing and Bioinformatics Analyses

383 PCR was performed on cDNA using Q5 High-Fidelity Polymerase (NEB). The K1 ORF was
384 amplified using primers M1_F1 or M1_F5 and M1_R6 (Table S3). The M1 region downstream of the

385 polyA stretch was amplified using M1_F7 and M1_R3. The LA virus was amplified using LA_F2 and
386 LA_R2, LA_F2 and LA_R3, or LA_F3 and LA_R6. PCR products were Sanger sequenced by Genscript.
387 Mutations were identified and peak height quantified using 4Peaks (nucleobytes). For
388 intracellular competitions, mutation frequency was quantified by both Sanger and Illumina sequencing
389 (see below), with both methods producing nearly identical results (Fig. S8).
390 The Sanger sequencing data was aligned to publicly-available M1 and LA references (GenBank
391 Accession Numbers U78817 and J04692, respectively) using ApE (A plasmid Editor). The ancestral M1
392 and LA viruses differed from the references at 7 sites (including 3 K1 missense mutations) and 19 sites,
393 respectively (Fig. S3).
394 Viral Transfer
395 Viruses were transferred to *MAT***a** strains using the *MAT*α karyogamy mutant as an intermediate.
396 Viral donors (*MAT***a**, *ura3,* NatMX) were first transformed with the pRS426 (*URA3*, 2μ ORI) for future
397 indication of viral transfer. Cytoduction was performed by mixing a viral donor with the karyogamy
398 mutant recipient (*MAT*α, *ura3*, KanMX) at a 5:1 ratio on solid media. After a 6 hr incubation at 30°C, the
399 cells were plated on media containing G418 to select for cells with the recipient nuclei. Recipients that
400 grew on -Ura (indicator of cytoplasmic mixing) and failed to grow on ClonNat (absence of donor nuclei)
401 then served as donors for the next cytoduction. These karyogamy mutant donors (*MAT*α, *URA3*, KanMX)
402 were mixed with the selected recipient (*MAT***a**, *ura3,* NatMX) at a 5:1 ratio on solid media. After a 6 hr
403 incubation at 30°C, the cells were plated on media containing ClonNat to select for cells with recipient
404 nuclei. Recipients that grew on -Ura (indicator of cytoplasmic mixing) and failed to grow on ClonNat
405 (absence of the donor nucleus) were then cured of the indicator plasmid by selection on 5-FOA. Killer
406 phenotype was confirmed by halo assays and the presence of the viral variants in the recipient was
407 verified by Sanger sequencing.
408 Illumina Sequencing and Bioinformatics Analyses
409 Multiplexed libraries were prepared using a two-step PCR. First, cDNA was amplified by Q5
410 High-Fidelity Polymerase (NEB) for 10 cycles using primers I292M_read1 and I292M_read2 or

411 frameshift_read1 and frameshift_read2 (Table S3) to incorporate a random 8 bp barcode and sequencing
412 primer binding sites. The resulting amplicons were further amplified by Q5 PCR for 15 cycles using
413 primers i5_adapter and i7_adapter to incorporate the sequencing adaptors and indices. Libraries were
414 sequenced on a NovaSeq 6000 (Illumina) at the Genomics Core Facility at Princeton University.

415 Raw FASTQ files were demultiplexed using a dual-index barcode splitter
416 (https://bitbucket.org/princeton_genomics/barcode_splitter) and trimmed using Trimmomatic (Bolger et
417 al. 2014) with default settings for paired-end reads. Mutation frequencies were determined by counting
418 the number of reads that contain the ancestral or evolved allele (mutation flanked by five nucleotides).

419 Intracellular Competitions

420 Within-cell viral competitions were performed by propagating a heteroplasmic diploid and
421 monitoring killer phenotype and viral variant frequency. Diploids were generated by crossing the ancestor
422 with a cytoductant harboring either the I292M or -1 frameshift viral variant. For each viral variant, three
423 diploid lines (each initiated by a unique mating event) were passaged every other day on buffered YPD
424 media for a total of 7 single-cell bottlenecks to minimize among-cell selection. A portion of each
425 transferred colony was cryopreserved in 15% glycerol. Cryosamples were revived, assayed for killer
426 phenotype, and harvested for RNA. Following RT-PCR, samples were sent for Sanger sequencing and
427 Illumina sequencing. Variant frequency deviated from the expected frequency of 0.5 at the initial
428 timepoint, presumably due to an unavoidable delay between the formation of the heteroplasmic diploid
429 and initiation of the intracellular competition from a single colony. Alternatively, viral copy number may
430 vary between donor and recipient cells.

431

432 **References**

433

434 Allesina, S. and J. M. Levine (2011). "A competitive network theory of species diversity." Proceedings of
435 the National Academy of Sciences **108**(14): 5638-5642.

436 Barrick, J. E. and R. E. Lenski (2013). "Genome dynamics during experimental evolution." Nat Rev
437 Genet **14**(12): 827-839.

438 Beaumont, H. J., J. Gallie, C. Kost, G. C. Ferguson and P. B. Rainey (2009). "Experimental evolution of
439 bet hedging." Nature **462**(7269): 90-93.

440 Bolger, A. M., M. Lohse and B. Usadel (2014). "Trimmomatic: a flexible trimmer for Illumina sequence
441 data." Bioinformatics **30**(15): 2114-2120.

442 Bostian, K. A., S. Jayachandran and D. J. Tipper (1983). "A glycosylated protoxin in killer yeast: models
443 for its structure and maturation." Cell **32**(1): 169-180.

444 Buskirk, S. W., R. E. Peace and G. I. Lang (2017). "Hitchhiking and epistasis give rise to cohort
445 dynamics in adapting populations." Proceedings of the National Academy of Sciences **114**(31): 8330-
446 8335.

447 Chao, L. and B. R. Levin (1981). "Structured habitats and the evolution of anticompetitor toxins in
448 bacteria." Proceedings of the National Academy of Sciences **78**(10): 6324-6328.

449 Crabtree, A. M., E. A. Kizer, S. S. Hunter, J. T. Van Leuven, D. D. New, M. W. Fagnan and P. A.
450 Rowley (2019). "A rapid method for sequencing double-stranded RNAs purified from yeasts and the
451 identification of a potent K1 killer toxin isolated from *Saccharomyces cerevisiae*." Viruses **11**(1): 70.

452 Daugherty, M. D. and H. S. Malik (2012). "Rules of engagement: molecular insights from host-virus arms
453 races." Annual review of genetics **46**: 677-700.

454 Dawkins, R. (1997). Human chauvinism, Evolution **51**: 1015-1020.

455 de Visser, J. A. G. and R. E. Lenski (2002). "Long-term experimental evolution in *Escherichia coli*. XI.
456 Rejection of non-transitive interactions as cause of declining rate of adaptation." BMC Evolutionary
457 Biology **2**(1): 19.

458 Diamond, M., J. Dowhanick, M. Nemeroff, D. Pietras, C. Tu and J. Bruenn (1989). "Overlapping genes in
459 a yeast double-stranded RNA virus." Journal of virology **63**(9): 3983-3990.

460 Esteban, R. and R. B. Wickner (1988). "A deletion mutant of LA double-stranded RNA replicates like M1
461 double-stranded RNA." Journal of virology **62**(4): 1278-1285.

462 Fisher, K. J., S. W. Buskirk, R. C. Vignogna, D. A. Marad and G. I. Lang (2018). "Adaptive genome
463 duplication affects patterns of molecular evolution in *Saccharomyces cerevisiae*." PLoS genetics **14**(5):
464 e1007396.

465 Frenkel, E. M., M. J. McDonald, J. D. Van Dyken, K. Kosheleva, G. I. Lang and M. M. Desai (2015).
466 "Crowded growth leads to the spontaneous evolution of semistable coexistence in laboratory yeast
467 populations." Proceedings of the National Academy of Sciences **112**(36): 11306-11311.

468 Georgieva, B. and R. Rothstein (2002). "Kar-mediated plasmid transfer between yeast strains: alternative
469 to traditional transformation methods." Methods in enzymology: 278-289.

470 Gerrish, P. J. and R. E. Lenski (1998). "The fate of competing beneficial mutations in an asexual
471 population." Genetica **102**: 127.

472 Gilpin, M. E. (1975). "Limit Cycles in Competition Communities." The American Naturalist **109**(965):
473 51-60.

474 Gould, S. J. (1985). "The paradox of the first tier: an agenda for paleobiology." Paleobiology **11**(1): 2-12.

475 Gould, S. J. (1996). Full House: The Spread of Excellence from Plato to Darwin. New York, Harmony
476 Books.

477 Gould, S. J. (1997). Self-help for a hedgehog stuck on a molehill, Evolution **51**: 1020-1023.

478 Greig, D. and M. Travisano (2008). "Density-dependent effects on allelopathic interactions in yeast."
479 Evolution: International Journal of Organic Evolution **62**(3): 521-527.

Gresham, D., M. M. Desai, C. M. Tucker, H. T. Jenq, D. A. Pai, A. Ward, C. G. DeSevo, D. Botstein and M. J. Dunham (2008). "The repertoire and dynamics of evolutionary adaptations to controlled nutrient-limited environments in yeast." PLoS genetics **4**(12).

Helling, R. B., C. N. Vargas and J. Adams (1987). "Evolution of *Escherichia coli* during growth in a constant environment." Genetics **116**(3): 349-358.

Holland, J., K. Spindler, F. Horodyski, E. Grabau, S. Nichol and S. VandePol (1982). "Rapid evolution of RNA genomes." Science **215**(4540): 1577-1585.

Icho, T. and R. B. Wickner (1989). "The double-stranded RNA genome of yeast virus LA encodes its own putative RNA polymerase by fusing two open reading frames." Journal of Biological Chemistry **264**(12): 6716-6723.

Jackson, J. and L. Buss (1975). "Alleopathy and spatial competition among coral reef invertebrates." Proceedings of the National Academy of Sciences **72**(12): 5160-5163.

Kane, W., D. Pietras and J. Bruenn (1979). "Evolution of defective-interfering double-stranded RNAs of the yeast killer virus." Journal of virology **32**(2): 692-696.

Károlyi, G., Z. Neufeld and I. Scheuring (2005). "Rock-scissors-paper game in a chaotic flow: The effect of dispersion on the cyclic competition of microorganisms." Journal of theoretical biology **236**(1): 12-20.

Kerr, B., M. A. Riley, M. W. Feldman and B. J. Bohannan (2002). "Local dispersal promotes biodiversity in a real-life game of rock–paper–scissors." Nature **418**(6894): 171-174.

Kirkup, B. C. and M. A. Riley (2004). "Antibiotic-mediated antagonism leads to a bacterial game of rock–paper–scissors in vivo." Nature **428**(6981): 412-414.

Kvitek, D. J. and G. Sherlock (2011). "Reciprocal sign epistasis between frequently experimentally evolved adaptive mutations causes a rugged fitness landscape." PLoS genetics **7**(4).

Kvitek, D. J. and G. Sherlock (2013). "Whole genome, whole population sequencing reveals that loss of signaling networks is the major adaptive strategy in a constant environment." PLoS genetics **9**(11).

Laird, R. A. and B. S. Schamp (2006). "Competitive intransitivity promotes species coexistence." The American Naturalist **168**(2): 182-193.

Lang, G. I., D. Botstein and M. M. Desai (2011). "Genetic variation and the fate of beneficial mutations in asexual populations." Genetics **188**(3): 647-661.

Lang, G. I., D. P. Rice, M. J. Hickman, E. Sodergren, G. M. Weinstock, D. Botstein and M. M. Desai (2013). "Pervasive genetic hitchhiking and clonal interference in forty evolving yeast populations." Nature **500**(7464): 571-574.

Liao, M. J., M. O. Din, L. Tsimring and J. Hasty (2019). "Rock-paper-scissors: Engineered population dynamics increase genetic stability." Science **365**(6457): 1045-1049.

Marad, D. A., S. W. Buskirk and G. I. Lang (2018). "Altered access to beneficial mutations slows adaptation and biases fixed mutations in diploids." Nature ecology & evolution **2**(5): 882-889.

May, R. M. and W. J. Leonard (1975). "Nonlinear aspects of competition between three species." SIAM journal on applied mathematics **29**(2): 243-253.

Menezes, J., B. Moura and T. Pereira (2019). "Uneven rock-paper-scissors models: Patterns and coexistence." EPL (Europhysics Letters) **126**(1): 18003.

Otto, S. P. and M. C. Whitlock (1997). "The probability of fixation in populations of changing size." Genetics **146**(2): 723-733.

521 Pagé, N., M. Gérard-Vincent, P. Ménard, M. Beaulieu, M. Azuma, G. J. Dijkgraaf, H. Li, J. Marcoux, T.
522 Nguyen and T. Dowse (2003). "A *Saccharomyces cerevisiae* genome-wide mutant screen for altered
523 sensitivity to K1 killer toxin." Genetics **163**(3): 875-894.

524 Paquin, C. E. and J. Adams (1983). "Relative fitness can decrease in evolving asexual populations of *S.*
525 *cerevisiae*." Nature **306**(5941): 368-371.

526 Petraitis, P. S. (1979). "Competitive networks and measures of intransitivity." The American Naturalist
527 **114**(6): 921-925.

528 Pieczynska, M., R. Korona and J. De Visser (2017). "Experimental tests of host–virus coevolution in
529 natural killer yeast strains." Journal of evolutionary biology **30**(4): 773-781.

530 Pieczynska, M. D., J. A. G. de Visser and R. Korona (2013). "Incidence of symbiotic dsRNA
531 'killer'viruses in wild and domesticated yeast." FEMS yeast research **13**(8): 856-859.

532 Pieczynska, M. D., D. Wloch-Salamon, R. Korona and J. A. G. de Visser (2016). "Rapid multiple-level
533 coevolution in experimental populations of yeast killer and nonkiller strains." Evolution **70**(6): 1342-
534 1353.

535 Plucain, J., T. Hindré, M. Le Gac, O. Tenaillon, S. Cruveiller, C. Médigue, N. Leiby, W. R. Harcombe, C.
536 J. Marx and R. E. Lenski (2014). "Epistasis and allele specificity in the emergence of a stable
537 polymorphism in *Escherichia coli.*" Science **343**(6177): 1366-1369.

538 Precoda, K., A. P. Allen, L. Grant and J. S. Madin (2017). "Using traits to assess nontransitivity of
539 interactions among coral species." The American Naturalist **190**(3): 420-429.

540 Rainey, P. B. and M. Travisano (1998). "Adaptive radiation in a heterogeneous environment." Nature
541 **394**(6688): 69-72.

542 Reichenbach, T., M. Mobilia and E. Frey (2007). "Mobility promotes and jeopardizes biodiversity in
543 rock–paper–scissors games." Nature **448**(7157): 1046-1049.

544 Ribas, J. C., T. Fujimura and R. B. Wickner (1994). "Essential RNA binding and packaging domains of
545 the Gag-Pol fusion protein of the LA double-stranded RNA virus of *Saccharomyces cerevisiae*." Journal
546 of Biological Chemistry **269**(45): 28420-28428.

547 Ribas, J. C. and R. B. Wickner (1992). "RNA-dependent RNA polymerase consensus sequence of the LA
548 double-stranded RNA virus: definition of essential domains." Proceedings of the National Academy of
549 Sciences **89**(6): 2185-2189.

550 Ridley, S. P. and R. B. Wickner (1983). "Defective interference in the killer system of *Saccharomyces*
551 *cerevisiae*." Journal of virology **45**(2): 800-812.

552 Rodríguez-Cousiño, N., P. Gómez and R. Esteban (2017). "Variation and distribution of LA helper
553 totiviruses in *Saccharomyces sensu stricto* yeasts producing different killer toxins." Toxins **9**(10): 313.

554 Rojas-Echenique, J. and S. Allesina (2011). "Interaction rules affect species coexistence in intransitive
555 networks." Ecology **92**(5): 1174-1180.

556 Rowley, P. A. (2017). "The frenemies within: viruses, retrotransposons and plasmids that naturally infect
557 Saccharomyces yeasts." Yeast **34**(7): 279-292.

558 Ruse, M. (1993). "Evolution and progress." Trends in ecology & evolution **8**(2): 55-59.

559 Schmitt, M. J. and F. Breinig (2002). "The viral killer system in yeast: from molecular biology to
560 application." FEMS microbiology reviews **26**(3): 257-276.

561 Schmitt, M. J. and F. Breinig (2006). "Yeast viral killer toxins: lethality and self-protection." Nature
562 Reviews Microbiology **4**(3): 212-221.

563 Shanahan, T. (2000). "Evolutionary progress?" BioScience **50**(5): 451-459.

564 Sinervo, B. and C. M. Lively (1996). "The rock–paper–scissors game and the evolution of alternative
565 male strategies." Nature **380**(6571): 240-243.

566 Soliveres, S., F. T. Maestre, W. Ulrich, P. Manning, S. Boch, M. A. Bowker, D. Prati, M. Delgado-
567 Baquerizo, J. L. Quero and I. Schöning (2015). "Intransitive competition is widespread in plant
568 communities and maintains their species richness." Ecology letters **18**(8): 790-798.

569 Spencer, C. C., J. Tyerman, M. Bertrand and M. Doebeli (2008). "Adaptation increases the likelihood of
570 diversification in an experimental bacterial lineage." Proceedings of the National Academy of Sciences
571 **105**(5): 1585-1589.

572 Suzuki, G., J. S. Weissman and M. Tanaka (2015). "[KIL-d] protein element confers antiviral activity via
573 catastrophic viral mutagenesis." Molecular cell **60**(4): 651-660.

574 Turner, P. E., V. Souza and R. E. Lenski (1996). "Tests of ecological mechanisms promoting the stable
575 coexistence of two bacterial genotypes." Ecology **77**(7): 2119-2129.

576 Van den Bergh, B., T. Swings, M. Fauvart and J. Michiels (2018). "Experimental design, population
577 dynamics, and diversity in microbial experimental evolution." Microbiol. Mol. Biol. Rev. **82**(3): e00008-
578 00018.

579 Wickner, R. B. (1976). "Killer of *Saccharomyces cerevisiae*: a double-stranded ribonucleic acid plasmid."
580 Bacteriological reviews **40**(3): 757.

581 Woods, D. and E. Bevan (1968). "Studies on the nature of the killer factor produced by *Saccharomyces*
582 *cerevisiae*." Microbiology **51**(1): 115-126.

583

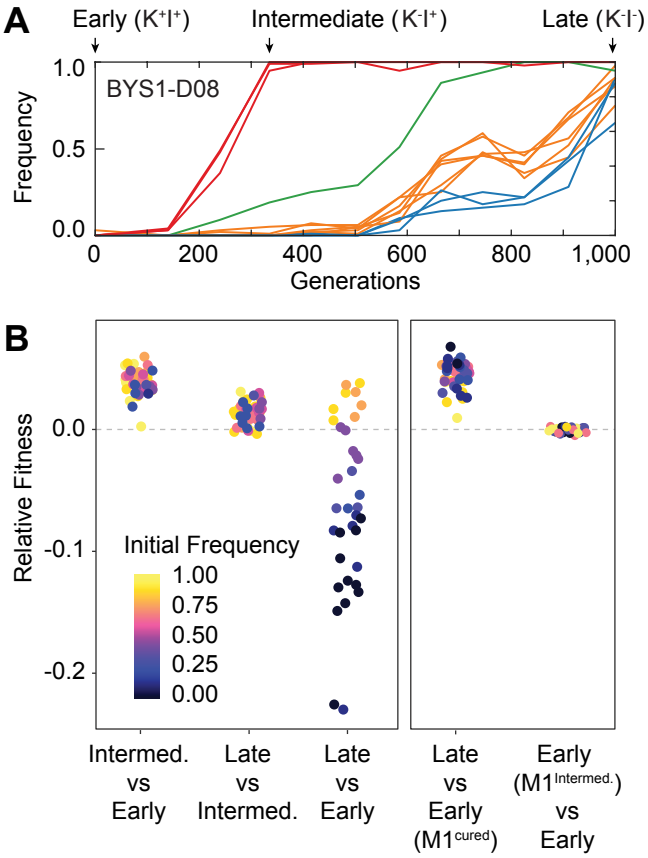

Fig. 1. Nontransitivity and positive frequency dependence arise along an evolutionary lineage. A) Sequence evolution (from Lang *et al*. 2013) shows that population BYS1-D08 underwent four clonal replacements over 1,000 generations. Mutations in the population that went extinct are not shown. The four selective sweeps are color-coded: red, mutations in *yur1*, *rxt2*, and an intergenic mutation; green, a single intergenic mutation; orange, mutations in *mpt5*, *gcn2*, *iml2*, *ste4*, *mud1*, and an intergenic mutation; blue, three intergenic mutations. The Intermediate clone, isolated at Gen. 335 does not produce, but is resistant to, the killer toxin (K-I+). The Late clone, isolated at Generation 1,000 does not produce, and is sensitive to, the killer toxin (K-I-). B) Competition experiments demonstrate nontransitivity and positive frequency-dependent selection. Left: Relative fitness of Early (Gen. 0), Intermediate (Gen. 335), and Late (Gen. 1,000) clones. Right: Relative fitness of the Early clone without ancestral virus or with the viral variant from the Intermediate clone. Fitness and starting frequency correspond to the later clone relative to the earlier clone during pairwise competitions.

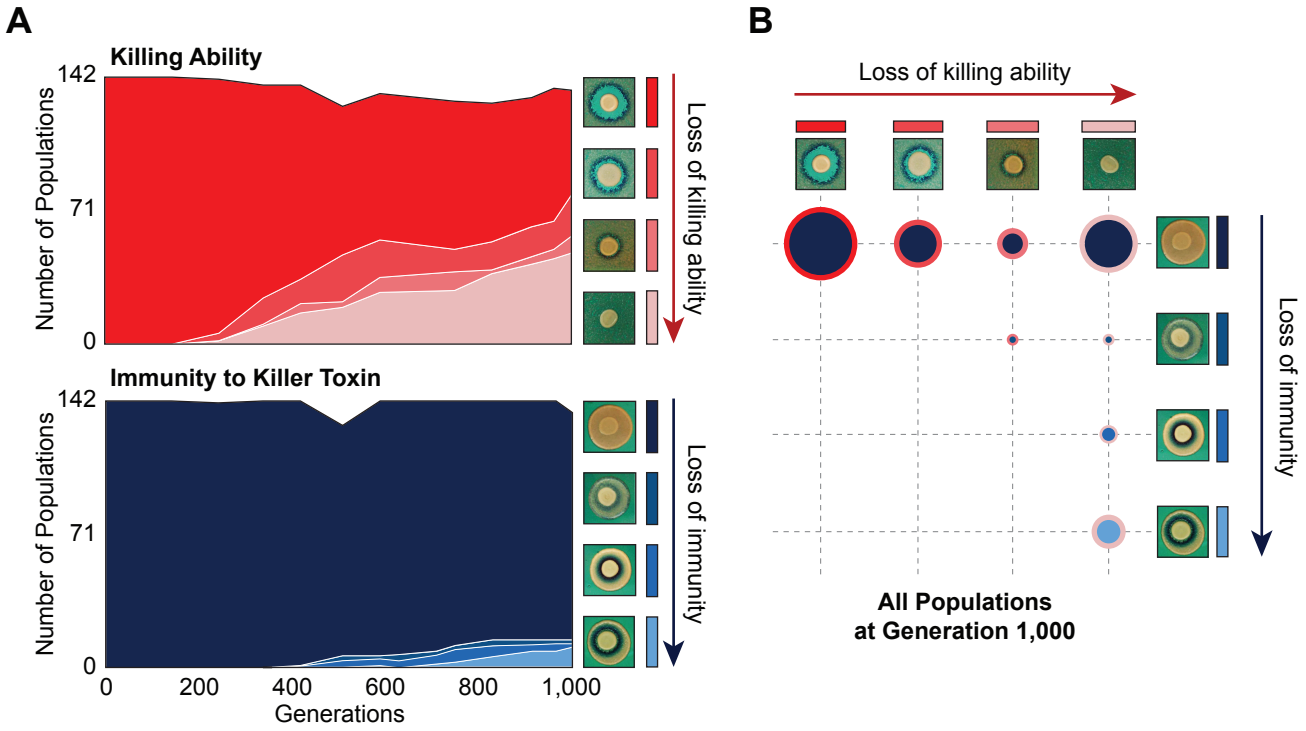

Fig. 2. Changes in killer-associated phenotypes in the 142 populations that were founded by a single ancestor and propagated at the same bottleneck size as BYS1-D08 (Lang *et al*. 2011). A) Loss of killing ability (top) and immunity (bottom) from evolving yeast populations over time. Killer phenotypes were monitored by halo assay (examples shown on right). B) Breakdown of killer phenotypes for all populations at Generation 1,000. Data point size corresponds to number of populations. Border and fill color indicate killing ability and immunity phenotypes, respectively, as in panel A.

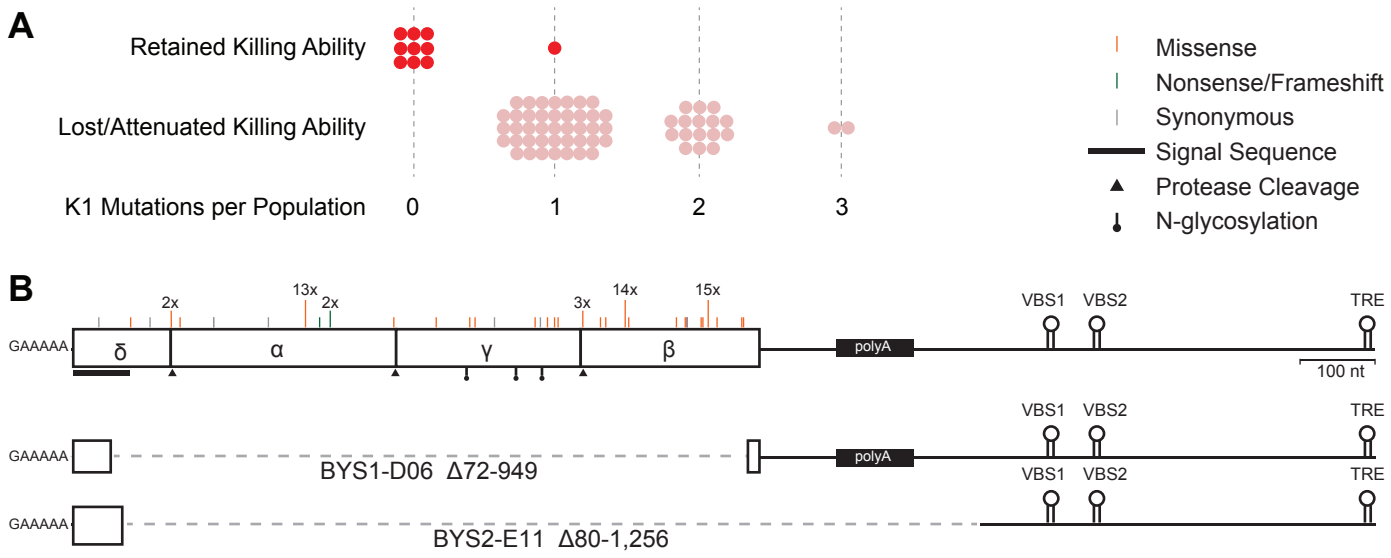

Fig. 3. Loss of killer phenotype correlates with presence of mutations in the K1 toxin gene. A) Number of mutations in the K1 gene in yeast populations that retain or lose killing ability. Each data point represents a single yeast population. B) Observed spectrum of point mutations across the K1 toxin in 67 evolved yeast populations. Mutations were detected in a single population unless otherwise noted. Large internal deletion variants from two yeast populations (BYS1-D06 and BYS2-E11). The deletions span the region indicated by the dashed gray line. VBS: viral binding site. TRE: terminal recognition element.

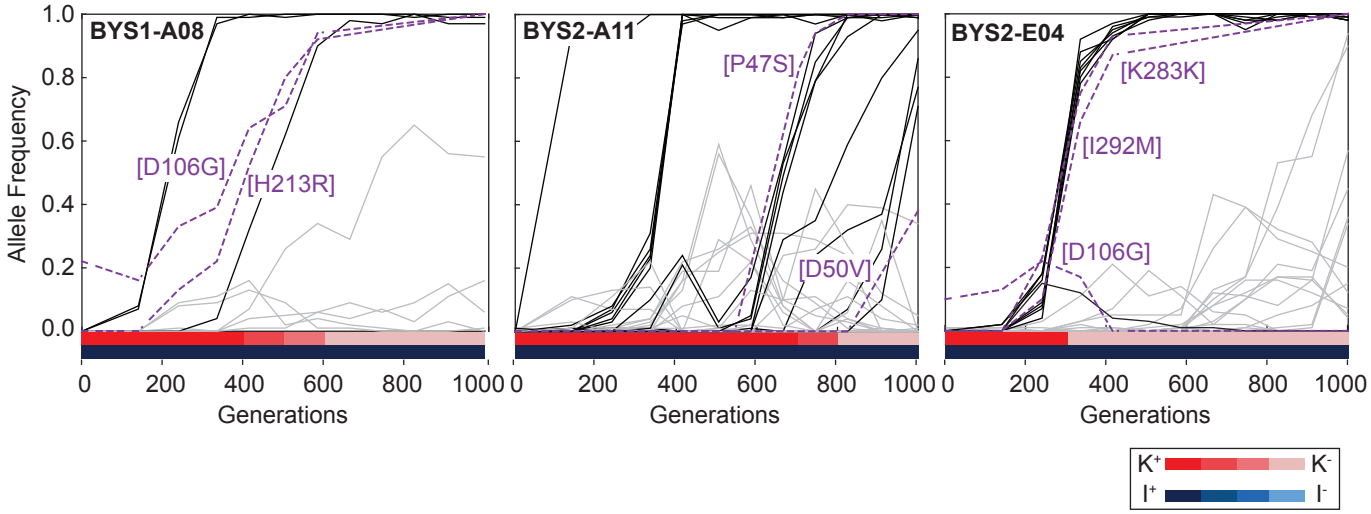

Fig. 4. Viral dynamics mimic nuclear dynamics. Killer phenotype of evolved populations is indicated by color according to the key. Nuclear dynamics (reported previously Lang et al 2014) are represented as solid lines. Nuclear mutations that sweep before or during the loss of killing ability are indicated by black lines. All other mutations are indicated by gray lines. Viral mutations are indicated by purple dashed lines and labeled by amino acid change.

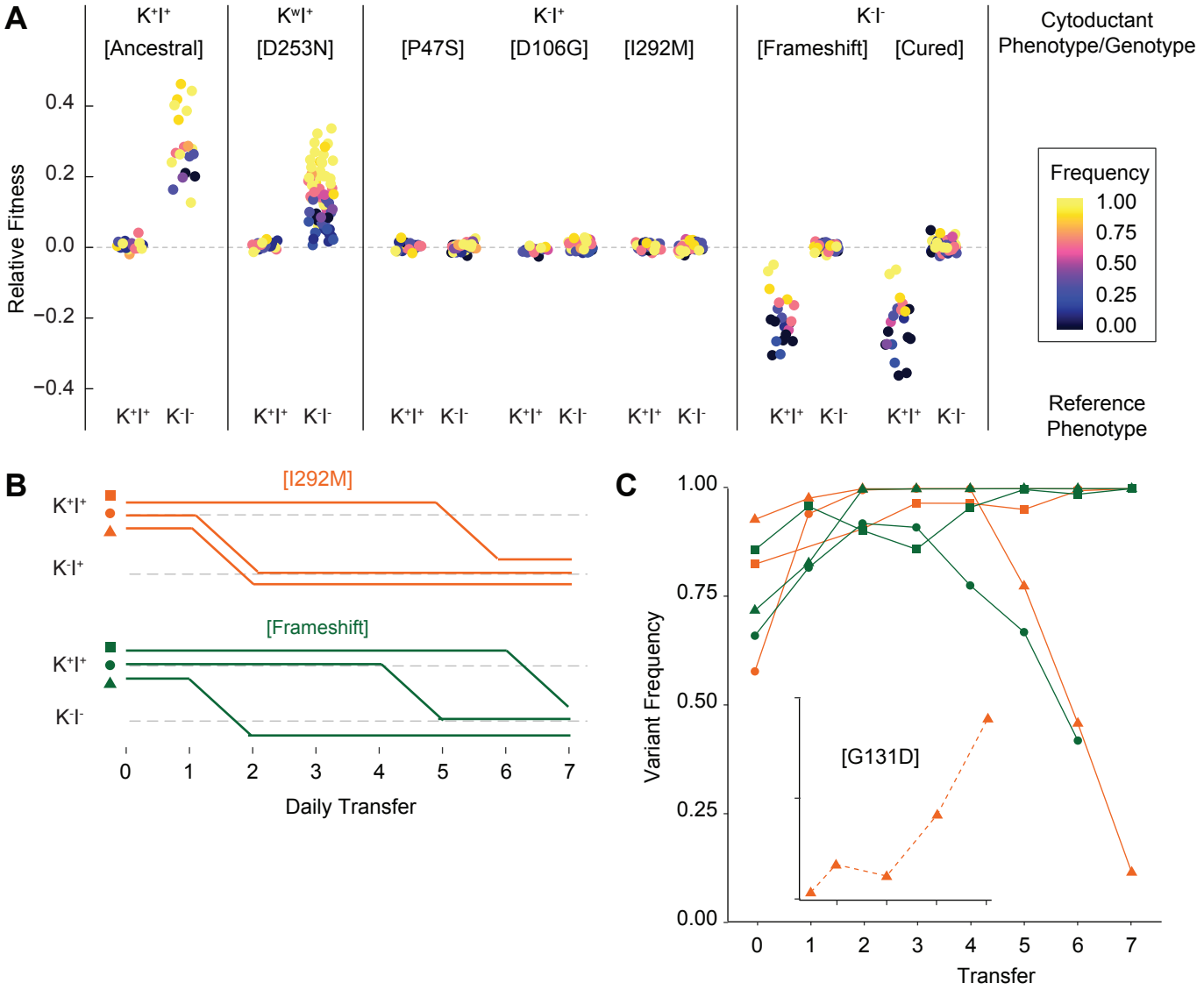

Fig. 5. Viral evolution is driven by selection for an intracellular competitive advantage. A) Relative fitness of viral variants in pairwise competition with the ancestor (K^+I^+) and virus-cured ancestor (K^-I^-). Killer phenotype and identity of viral variant labeled above (K^w indicates weak killing ability). Killer phenotype of the ancestral competitor labeled below. Starting frequency indicated by color. B) Change to killer phenotype during intracellular competitions between viral variants (by color) and ancestral virus. Replicate lines indicated by symbol. C) Variant frequency during intracellular competitions. Colors and symbols consistent with panel B. Inset: frequency of the de novo G131D viral variant.